Investigation of the Impact of Thermal Spraying with Diverse Ceramic Powders on the Sliding Corrosion Resistance of (AISI 446) Steel Alloys

Authors Names

Ahmed Subhi Ali Husseina[a]

Yaha Abdulkareem AL Salman[b]

EdreesE. Khadeer[c]

Publication date: 20 /8 /2025

Keywords: . Alloys, Sliding corrosion resistance, Thermal spraying

Abstract

According to this study, the sliding wear resistance of (AISI446) stainless steel alloy thermally coated with various ceramic powders such as silicon oxide and carbide ($SiC + SiO_2$)and at different weight concentrations was studied, obtaining these coatings with a (QH-2/H thermal spray) welding torch. In order to assess these coatings' performance, The test for sliding wear resistance was carried out. using a pin-on-dish sliding wear tester designed according to (ASTM D5963) specifications under variable vertical loads, speeds or surfaces. The testing results indicated the efficiency of these coatings in enhancing the erosion resistance to sliding wear of the various covered alloys in contrast to the base alloy that isn't coated. All of the samples that were evaluated showed a gradual rise in wear rate as the loads increased. It was also discovered that the alloy (F_2)which contained silicon carbide at a rate of (100%) and the binder material (Ni-Al), displayed the lowest corrosion rate compared to the coated and uncoated alloys. Additionally, compared to the basic alloy, this alloy's corrosion rate dropped by 54.70% under the load (26N), however the coated sample (F_4) consisting of silicon carbide and a percentage of (80 wt. %SiC+20 wt. % SiO_2) The highest wear rate of the uncoated alloy base with an improvement rate of -)53.96%(. The alloy (F_4), including 80% silicon carbide (SiC) and (20%) silicon oxide (SiO_2), had the lowest sliding wear rate at a speed of (180 rev/min), demonstrating an improvement rate of (74.14%). Although the abrasive surface exhibited significant enhancements in sliding wear resistance the coated sample (F_4) exhibited higher wear rates than the uncoated base alloy at varying percentages in comparison to the uncoated base alloy, with a rate of (-109.49%).

1.Introduction

Thermal spraying technology has been used in many modern industries to apply a coating to surfaces by pushing molten or semi-molten materials, which enhances the properties of the surface to be coated. This technology is used with a variety of materials, including metals, alloys and ceramics, and is applied to many metals and alloys, such as stainless steel alloys of various types, which gives them excellent resistance to mechanical and chemical corrosion such as oxidation at temperatures up to and makes them suitable for use in many thermal applications such as steam generators and furnace parts [1]. Surface studies have received great attention in many industrial applications that change the surface of the manufactured metal or alloy to achieve specific properties. This modification of the surface occurs in various ways, often using heat treatments or chemical heat to achieve precise modifications or diffusion of material molecules such as carbon and nitrogen [2]. It is possible to obtain surface properties different from the base uncoated alloy. Thermal spraying techniques depend on the thermal or kinetic energy of the melted raw material and the method of pushing it into the base

[a]University of Mosul, College of Science, Department of Physics, Mosul, Iraq, E-Mail: ahmed.scp99@student.uomosul.edu.iq
[b] University of Mosul, College of Science, Department of Physics, Mosul, Iraq, E-Mail: Yahya200138@uomosul.edu.iq
[c] University of Mosul, College of Science, Department of Physics, Mosul, Iraq, E-Mail: dr.address@uomosul.edu.iq

alloy as well as the form of particles or droplets of the spray material. Many materials can be thermally sprayed, according to the compatibility between the specific process and the materials [3]. The mechanical and physical characteristics of coated materials, including strength, hardness, fatigue life, corrosion resistance, insulation, and thermal conductivity, are different from those of their uncoated components [4]. Numerous researchers have concentrated on enhancing iron alloys' mechanical characteristics and increasing their ability to resist friction and corrosion. The results showed that the rate of erosion corrosion increases linearly with many variables such as vertical sliding distance, linear velocity, and the nature of the abrasive surface [5]. The experimental results also showed that the corrosion rate also increases with the increase of other factors such as humidity, heat generated as a result of the friction process, sliding distance, and applied load [6]. Therefore, these studies recommended the need to ensure the selection of appropriate materials and coating methods to enhance corrosion resistance.

2. Experimental Part

2.1 Material selection

The AISI446 stainless steel alloy was chosen as the base alloy because it is used in the oil industry, power generation equipment and chemical processing, due to its distinctive properties in resisting corrosion and oxidation at high temperatures, as it can be placed in thermal environments for a long time without losing its mechanical properties in addition to its resistance to corrosion resulting from erosion and erosion (wear and crosin). Table (1) shows the weight percentages of the base alloy (AISI 446).

Table (1): Weight ratios of stainless steel alloy (AISI 446) [7]

Alloy designation	**The code of Sample**	**Chemical composition, weight percent**							
AISI 446	F_o	Fe	Cr	Mn	Yes	No	C	P	S
		73	23.0-27.0	1.50	1.0	0.25	0.20	0.040	0.030

Using Ni-Al powder as a bond coating consisting of (50 Al-50 Ni) which is characterized by its high ability to create immediate adhesion between the coating components on the one hand, and the coating and the base alloy on the other hand. Table (2) shows the basic components of the bond coating.

Table (2): Weight ratios of bond coating powder

Powder designation	Chemical equation	The code of Sample	Chemical composition, weight percent	
Bond coating	Ni-Al	F_1	Ni	Al
			50	50

Table (3) shows the weight percentages of ceramic powders used as thermal barrier coatings.

Table (3): Weight ratios of thermal barrier coating powder

Powder designation	Chemical equation	The code of Sample	Chemical composition, weight percent	
Thermal barrier coating	SiC_SiO_2		SiO_2	SiC
		F_2	20	80
		F_3	40	60
		F_4	60	40
		F_5	80	20
		F_6	100	0
		F_7	0	100

2.2 Sample Preparation

The sliding wear resistance test samples for AISI446 stainless steel alloy were designed as shown in Figure (1).

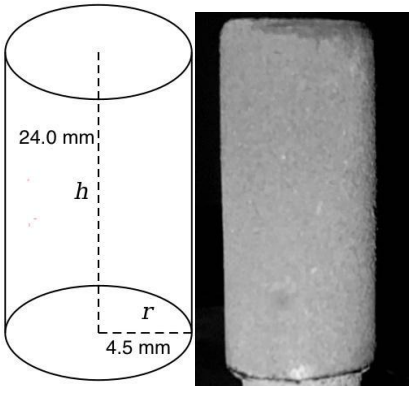

Figure Corrosion test sample1 :

This process includes several stages starting with roughening the samples using (320#) sandpaper, then washing with soap and water, then immersing them in an acetone solution using an ultrasonic cleaning

device for (480 sec) to remove any remaining impurities and contaminants, ensure the surface is pristine. Subsequently, they are rinsed with distilled water and rapidly dried using hot air, before being placed in sealed bags, rendering them prepared for the painting procedure.

2.3 Coating Processes

The flame spray system was designed and assembled from the local market as shown in Figure (2). The samples were fixed on an electric motor that rotates at a constant speed to maintain the uniform distribution of the paint on the part to be coated, and it is (12 cm) away from the nozzle of the thermal spray gun. The thermal gun is used to spray the powder placed in the crucible by pressing the regulators fixed in the body of the thermal gun so that a thermal flame is produced as a result of burning acetylene gas and oxygen gas in a stream that includes a mixture of the two gases. This gas stream carries the paint powder stored in the reservoir (tank) at the top of the spray gun to melt and flow smoothly and for the molten paint to adhere well to the surface of the samples. To obtain a constant rate for the mixture of gas and molten powder, the pressure of the oxygen gas should not exceed (4.07 Bar) and the pressure of the acetylene gas should not exceed (0.7 Bar). The spraying process begins by heating the sample for (10 sec) using an oxy-acetylene torch, and in order for the coating process to be completed on the surface of the sample to be coated, it takes (20 sec), then the samples are left in the air to cool. Figure (2) shows the spraying system used in the coating process.

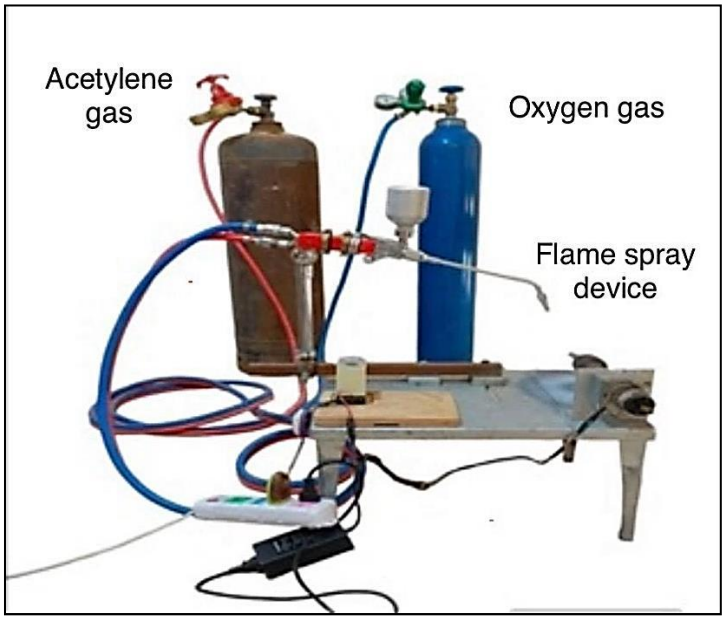

Figure 2: Thermal spray system

2.4 Thermal Spraying

The powder is sprayed with the flame resulting from mixing oxygen with acetylene. The flame can be controlled (increased or decreased) by changing the oxygen ratio. Then the Coating procedure begins, as shown in Figure (3b).

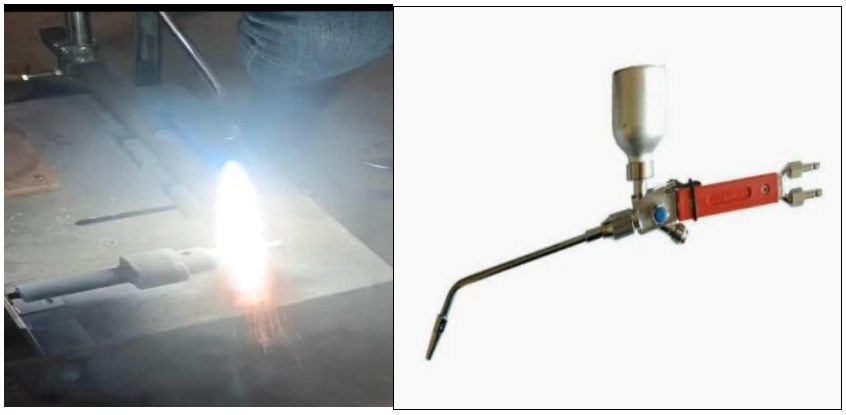

a b

Figure 3: a) Thermal spray torch, b) Coating procedure .

The coating process was carried out using a Chinese-made flame Spray welding torch model (QH-2/H) shown in Figure (2a). Table (4) shows the changes established in the thermal spraying process while maintaining the base alloy temperature within the range (before the spraying process, in order to avoid peeling during the final cooling stage.

Table (4) : The parameters of the thermal spraying procedure.

Mixing Oxy-Acetylene	4: 0.7 Bar
Flame spray temp	2500° C
Powder feeding	4.177 gm/min
Spraying distance	12 cm
powder particle size	25-75 μm
Time spent coating	10 to 20 sec

2.5 Sliding Wear Test

All of the samples intended for this purpose underwent the gravimetric approach for the slide wear test at room temperature to ascertain the mechanical wear rates that occur in both coated and untreated samples due to changes in the applied loads, speed, or nature of the abrasive surface. Necessary precautions were taken to reduce the testing period of the samples at each test, with the aim of

reducing the impact of temperature during sample testing, as it is thought to be one of the element influencing the sliding wear rate numbers that transpire.

The initial section involved applying many loads while fixing the friction disc's rotating speed (V), the sample's friction circle radius (r), the friction surface roughness, and the sliding time (t).

While the second part included changing the linear sliding speed, with the applied load fixed. The third part included changing the type of the abrasive surface with both the applied load and speed fixed, and the table shows the most important variables and constants that were performed on the samples during the test period.

Table (5) Sliding wear test parameters

Variable Friction Nature (100,180,240,320,400)#	**Variable Sliding Velocity (60,90,120,150,180)min/sec**	**Variable Load (10N,14N,18N,22N,26N)**
r = 20 mm , t = 300 sec V =120 min/sec, 320# Weight=18N	r = 20 mm , t = 300 sec 320# Weight=18N	r = 20 mm , t = 300 sec V =120 min/sec

A sliding wear apparatus designed according to ASTM D5963 specifications, with a screw-on-disc arrangement, was used. The aim of this arrangement is to achieve a direct contact condition between the cylindrical specimen and the revolving disc subjected to vertical load, which allows the study of wear effects under different conditions, as shown in Figure (4).

Figure 4: Corrosion testing device

The apparatus has a motor with adjustable speed. The apparatus features a steel arm affixed at one end to its body. The opposite end features a holder designed to secure the sample at its top section. To apply stresses to its upper section, which is secured at one end, it glides on the revolving disc; the wear rate is almost determined as follows [8]:

$$\Delta W = W_1 - W_2 \quad (1)$$

$$\text{Wear reat} = \frac{\Delta \text{W}}{\text{S}_\text{D}} \left[\frac{\text{gm}}{\text{cm}}\right] \quad (2)$$

Where:

ΔW: denotes the variation in mass (grammes)

W_1: sample mass before the test (gm)

W_2: sample mass after the test (gm)

S_D: The distance of sliding (cm) is articulated by the subsequent equation:

$$\text{S}_\text{D} = \text{t.v} \quad (3)$$

Where :

t: The time of sliding (seconds), v: sliding speed (cm/sec), derived from the following equation:

$$\text{V} = \pi DN \quad (4)$$

Where :

N: disk speed (rpm), D: sliding diameter (cm)

r: sliding radius (cm).

By substituting equations (3) and (4) in equation (2), we get:

$$\text{Wear reat } (W.R) = \frac{\Delta \text{W}}{(2\pi \text{r. t. N})/60} \quad (5)$$

3. Results and discussion

The wear rate for both the basic alloy and the coated variety increases as the applied load increases, according to the graphs showing the link between wear rate and changes in applied loads, which are shown in Figure (5). The increase in plastic deformation at the apex of the surface protrusions of the samples results in a heightened density of dislocations [9].

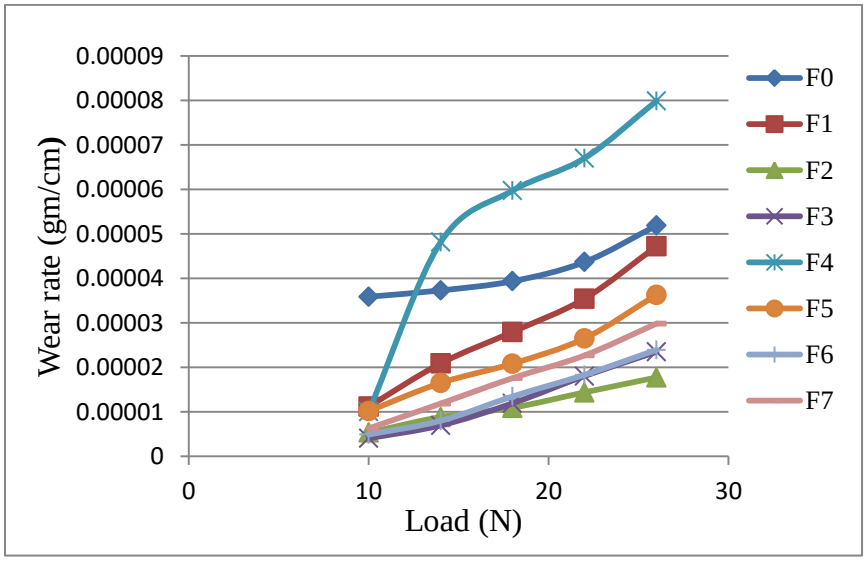

Figure (5): Sliding wear rate of coated and uncoated samples at different loads

This leads to an increase in the hardness of the material and it gradually becomes brittle, which causes an increase in the accumulation of dislocations and the formation of small gaps that unite to form small cracks on the surface of the alloy, whether coated or uncoated. The small cracks develop or expand and move under the influence of stresses towards weak areas, which leads to the formation of larger cracks as a result of their rapid accumulation. The convergence of these cracks contributes to the removal of thin layers of the alloy in the direction of the sliding movement, which results in wear debris particles, which are formed due to weariness or depletion in the outermost layers [10]. This process leads to the formation of a thin layer of oxide on the metal alloy due to the high temperature of the two contacting surfaces, which leads to covering the wear surface and reducing the friction process over time, and weather conditions exert a significant influence on the pace of oxide formation [11].

The three steps of the adhesion process between when the two sliding surfaces protrude are determined by the applied load. Initially, there is no real contact between the two contacting surfaces due to the formation of a thin layer of oxide at low loads. As a result, The force of the alloy atoms is greater than the force needed to break the link between the protrusions, which contributes to low corrosion rates due to the absence of the powdered oxide coming out of the sample surface. The first stage of weak corrosion is known as light corrosion [12].

It can be observed in Figure (5) at loading rates ranging from 10 to 14 N. With increasing loads, the oxide layer is exposed to fracture, resulting in a strong metallic connection. This connection requires a greater force to separate the connected protrusions compared to the force of the alloy atoms, which significantly increases the corrosion rates. The stage resulting from the increase in powdered oxide emitted from the sample is known as the transition corrosion stage, and can be observed at loading

rates ranging from 14 to 18 N [13]. While the severe corrosion stage is considered the final stage, and occurs at loading rates exceeding 22 N, where the alloys do not have enough time to form oxide, which leads to the removal of thin layers from the surface of the alloys themselves [14].

Comparing the rates of corrosion of samples covered with different kinds of ceramic powders, it was discovered that these rates vary depending on the type and concentration of coating powders used. The aforementioned stages explain the sliding corrosion behaviour of the uncoated basic alloys. In comparison to the coated and uncoated alloys, the coated sample (F_2) exhibited the lowest corrosion rate, as seen in the preceding figure. The corrosion rate of these alloys decreased by (-53.96%)when applying a load of 26 N, which represents more than half the corrosion rate of the uncoated alloys. This improvement in corrosion resistance is due to several factors, most notably that the coating gave the alloys higher hardness, which reduced the plastic deformation resulting from friction between the two surfaces [14]. As observed when the load was increased to (26N), the formed oxide layer was broken, resulting in a strong metal contact protrusion, which raises the wear rates considerably because it takes more force to cut or separate the attached protrusions than the alloy atoms' strength .

The lack of sliding wear equations is lessened by the reduction in both the actual contact area and shear force. When the coating is on one or both sides, the sliding becomes weaker because the broken coating layer during wear functions as a lubricant owing to the contact between the protrusions of the sliding surfaces. As a result, the wear rate is reduced since less shear force is needed [15]. In Table 6, it is clear that the samples coated demonstrated a notable increase in sliding wear resistance when compared to the basic alloy without any ceramic coatings.

Table 6: percentage increase in coated alloys' sliding wear under load (26N).

No.	Sample code	Improvement Percentage(%)	Load (N)
1	$F_\circ$	0	26
2	F_1	8.95	26
3	F_2	65.79	26
4	F_3	54.70	26
5	F_4	- 53.96	26
6	F_5	30.0	26
7	F_6	53.85	26
8	F_7	42.46	26

After the coating process, all samples were heat treated at a temperature of 900 °C, which increased the hardness of the alloy. Figure (6) shows that the coated alloy (F_4) consisting of 80% silicon carbide (SiC) powder and 20% silicon oxide powder (showed the lowest sliding wear rate compared to other samples). This suggests that the resistance to sliding wear has improved depending on the type of coating used as well as the adhesion strength to resist the alloy from corrosion due to the adhesion strength between the silicon carbide particles on the one hand and the base alloy in addition to the nickel-aluminum bonding material on the other hand, while the other coated alloys had a clear effect on corrosion at varying rates. Figure (7) shows the relationship between the linear sliding velocity and the sliding wear rate, where it was noted that the wear rate for all coated and uncoated samples gradually decreases with increasing linear sliding velocity. However, when comparing the sliding wear behavior when changing the concentration of coating powders, it was noted that there is a clear decrease in the sliding wear rate of The alloy The coated alloy (F_4) consisting of (60 wt%) and (40 wt%), which was the lowest compared to the rest of the coated and uncoated alloys, is due to the rapid erosion of the coating layers, which led to filling the voids or cavities formed by the sliding process due to the high sliding speed, forming a layer that isolates the alloy surface from the friction surface, which led to increased wear resistance and the adhesion of the separate coating particles as a result of the erosion process with the surface, while the coated alloy (F_1) consisting of the link coating showed the highest rates of sliding wear, and this comes as a result of the decrease in the strength of the bond between the coating layer and the base alloy, as a result of the distortion process. Because the heat generated during friction at low speeds is greater than in the case of high speeds, this leads to an increase in the softness of the protrusions at high speeds, It results in a reduction in the wear rate as the sliding speed increases because the force needed to cut the contact points is less than the bonding force of the alloy or covering metal atoms.

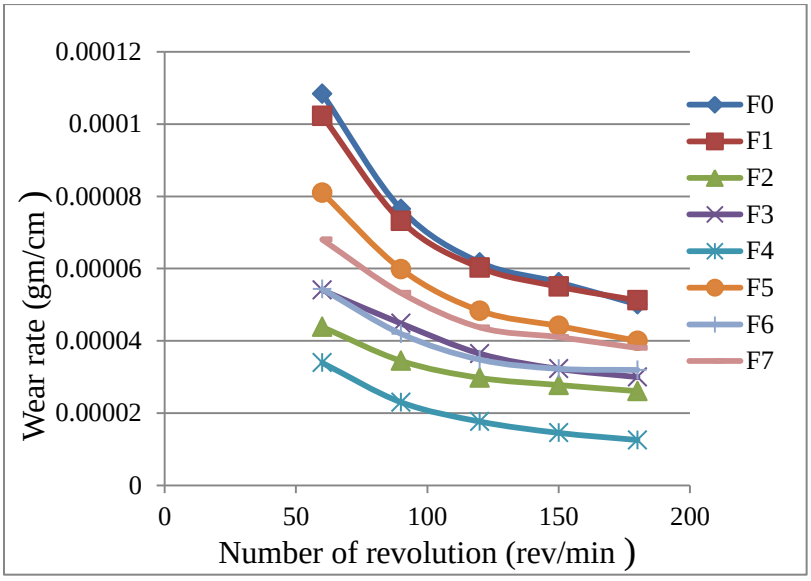

Figure (7): Sliding wear rate of coated and uncoated samples at different speeds

Comparing the other coated samples to the uncoated base alloy, Table 7 demonstrates a notable increase in sliding wear resistance. With a 2.25% improvement, the coated sample did, however, exhibit a greater wear rate than the untreated base alloy.

When performing the sliding wear test by changing the nature of the abrasive surface, by changing the friction surfaces, shown in Figure (8), it was found from the figure that the sliding wear rate decreases with increasing roughness of the granular surface [15]. The reason for this is due to the small number of granules present on the surface area of the paper or the abrasive surface, i.e. in other words, the smoother the granular surface of the abrasive surface, the greater the amount of wear [16].

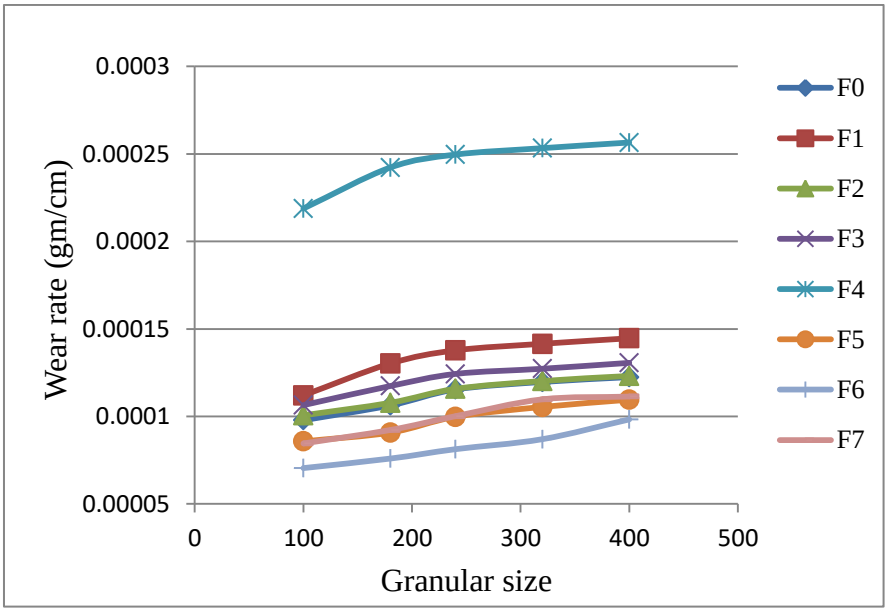

Figure (8): Sliding wear rate of coated and uncoated samples at different grain surfaces.

As for the samples coated with the remaining ceramic coatings, we note that they also showed a significant improvement in varying percentages with the exception of the coated sample (F_4), which, in terms of resistance to sliding wear, demonstrated higher wear rates than the uncoated base alloy by (-109.49%). , as seen in Table (8).

Table 8: percentage increase in coated alloys' sliding wear at a grain size of (400#) for the nature of the abrasive surface.

No.	Sample code	Improvement Percentage(%)	Grain size of friction surface (#)
1	F_1	-18.11	400
2	F_2	0.54	400
3	F_3	-6.65	400
4	F_4	-109.49	400
5	F_5	10.55	400
6	F_6	19.74	400
7	F_7	9.08	400

There are a number of reasons why the aforementioned alloys differ in their relative improvements in sliding wear resistance [16], including:

1- The type of ceramic powders that are utilised in the coatings : as they are manufactured using powder technology, which affects the properties of the materials.

2- Weight ratios: The weight ratios of the powders vary according to the composition, which affects the density and final hardness.

3- Alloy hardness: Adding powders enhances hardness and reduces the rate of wear, as these properties are inversely proportional to wear resistance.

4- Structural composition: The structural composition of the powders affects the temperature at which the sample and friction disc come into contact, which changes the softness of the sliding surfaces.

5- Defects: The wear behaviour of the coated alloys is adversely affected by the presence of defects like cracks and pores.

References

[1] Askeland DR, Phulé PP, Wright WJ, Bhattacharya DK. The science and engineering of materials. 2012.

[2] Bandar AA, Abbas MK, Tuaimah SK. Study of the mechanical properties and wear resistance of aluminum-glass composites. J Eng Technol 2012:2128

[3] Dzhurinskiy D, Babu A, Dautov S, Lama A, Mangrulkar M. Modification of cold-sprayed Cu-AlNi-Al2O3 composite coatings by friction stir technique to enhance wear resistance performance. Coatings 2022 Aug 4; 12(8):1113.

[4] Dzhurinskiy, D.; Babu, A.; Dautov, S.; Lama, A.; Mangrulkar, M. Modification of Cold-Sprayed Cu-Al-Ni-Al2O3 Composite Coatings by Friction Stir Technique to Enhance Wear Resistance Performance. Coatings 2022, 12, 1113. https:// doi.org/10.3390/coatings12081113 Received: 29 June 2022 Accepted: 28 July 2022 Published: 4 August 2022.

[5] Eyre TS. Wear characteristic of metal. Triobol Int 1976; 9:203-12

[6] Franco, D.; Ageorges, H.; Lopez, E.; Vargas, F. Tribological performance at high temperatures of alumina coatings applied by plasma spraying process onto a refractory material. Surf. Coat. Technol. 2019, 371, 276–286.

[7] Groover. ،M. P. (2007). Fundamentals of Modern Manufacturing. John Wiley & Sons, New York. OCLC:315203106.

[8] https://www.tritonalloysinc.com/446-stainless-steel-sheet.html

[9] Mazin A, Mahmood A, Gader EE. Effect of time on weight gain, thickness, cycle oxidation of thermal barrier coating (TBC) ZrO2 at super alloy IN738LC. Oxid Commun 2022 Jan 1; 45(1):186.

[10] Pulsford, C. (2022). Microstructure characterisation of long-term aged advanced austenitic stainless steels for power plant applications (Doctoral dissertation, Loughborough University).

[11] Rana N, Mahapatra MM, Jayaganthan R, Prakash S. Deposition of nanocrystalline coatings by modified LVOF thermal spray method. J Alloys Comp 2014 Dec 5; 615:779–83.

[12] Tao K, Zhou X, Cui H, Zhang J. Microhardness variation in heat-treated conventional and nanostructured NiCrC coatings prepared by HVAF spraying. Surf. Coat. Technol. 2009; 203; 1406–1414.

[13] Tsukizoe T, Ohmae N. Friction and wear of advanced composite materials. Fibre Sci Technol 1983; 18(4):265–86.

[14] Vafaeenezhad H, Zebarjad SM, Khaki JV. Fabrication and wear behavior investigation of the car bon/epoxy composites based on wood using artificial neural networks. Adv Mat Res 2012 Feb 20; 413:95–102.

[15] Venturi F, Pulsford J, Hussain T. A novel approach to incorporating graphene nanoplatelets into Cr2 O3 for low-wear coatings. Mat Lett 2020; 276:128–283.

[16] Wang BQ, Lee SW. Elevated temperature erosion of several thermal-sprayed coatings under the simulated erosion conditions of in-bed tubes in a fluidized bed combustor. Wear 1997; 203-204; 580-587.